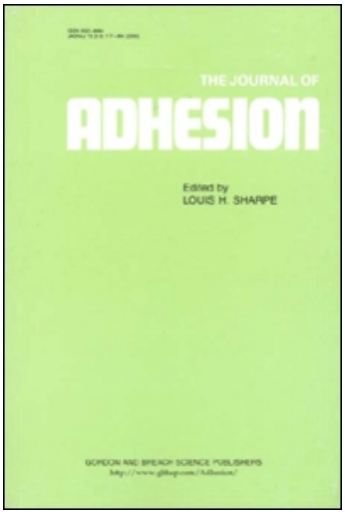

The Journal of Adhesion
Publication details, including instructions for authors and subscription information:
http://www.informaworld.com/smpp/title~content=t713453635

Adhesion of Graphite Fibers to Epoxy Matrices: II. The Effect of Fiber Finish

Lawrence T. Drzal[a]; Michael J. Rich[b]; Michael F. Koenig[b]; Pamela F. Lloyd[c]
[a] Air Force Wright Aeronautical Laboratories, Nonmetallic Materials Division, Mechanics and Surface Interaction Branch, AFWAL/MLBM Wright-Patterson Air Force Base, WPAFB, OH, U.S.A. [b] University of Dayton Research Institute, Dayton, Ohio, U.S.A. [c] Systems Research Laboratory, Dayton, Ohio, U.S.A.

To cite this Article Drzal, Lawrence T. , Rich, Michael J. , Koenig, Michael F. and Lloyd, Pamela F.(1983) 'Adhesion of Graphite Fibers to Epoxy Matrices: II. The Effect of Fiber Finish', The Journal of Adhesion, 16: 2, 133 — 152
To link to this Article: DOI: 10.1080/00218468308074911
URL: http://dx.doi.org/10.1080/00218468308074911

J. Adhesion, 1983, Vol. 16, pp. 133–152
0021–8464/83/1602–0133 $18.50/0

Printed in the United Kingdom

Adhesion of Graphite Fibers to Epoxy Matrices: II. The Effect of Fiber Finish

LAWRENCE T. DRZAL†

Air Force Wright Aeronautical Laboratories, Nonmetallic Materials Division, Mechanics and Surface Interaction Branch, AFWAL/MLBM Wright-Patterson Air Force Base, WPAFB, OH 45433, U.S.A.

MICHAEL J. RICH and MICHAEL F. KOENIG

University of Dayton Research Institute, Dayton, Ohio 45469, U.S.A.

and

PAMELA F. LLOYD

Systems Research Laboratory, 2800 Indian Ripple Road, Dayton, Ohio 45440, U.S.A.

(*Received March 9, 1983; in final form July 15, 1983*)

Reinforcing fibers are available from various manufacturers with matrix compatible "finishes" applied to them. Usually these finishes or coatings are 100–200 nm thick resin layers applied after surface treatment. Their function has been hypothesized as being to enhance adhesion through either protecting the fiber from handling damage, protecting the fiber surface reactivity, or improving fiber wettability. This study of finished and unfinished graphite fibers concludes that the mechanism by which an epoxy compatible finish operates is different from what has been hypothesized to date. The finish layer creates a brittle interphase layer between the fiber and matrix which increases the interfacial shear strength but at the expense of changing the failure mode from interfacial to matrix.

1. INTRODUCTION

The interface between fiber and matrix in composite materials is often

† To whom all correspondence should be addressed.

the controlling factor in obtaining optimum mechanical properties from the composite. Commercial composites have an optimized interface which efficiently transmits forces between fiber and matrix in a given material system. The actual mechanism by which the interface operates under chemical, mechanical, and thermal environments is not known but must be understood if the interface is to be optimized for new composite systems.

Reinforcing fibers are available not only with surface treatments designed to increase the chemical interaction between fiber and matrix but also with surface finishes or sizings applied to enhance compatability with the host matrix. Previously reported work[1] has clarified the role of the graphite fiber surface treatments. Surface treated graphite fibers can be obtained with "matrix compatible" finishes, for example. Usually these finishes are applied as very thin coatings (*e.g.*, 100–200nm) from solution. Compositionally they can vary from consisting of the pure resin component without a crosslinking agent and therefore unpolymerized to being a mixture of polymers partially crosslinked. The usual explanation for the use of these finishes is that they

a. Protect the fiber surface from damage
b. Improve the wetting of the fiber by the matrix
c. Protect fiber surface reactivity.[2,3]

The purpose of this study is to elucidate the mechanism by which surface finishes operate and to assess their effect on fiber-matrix adhesion.

2. EXPERIMENTAL

A. Fibers

Two polyacrylonitrile based graphite fibers were chosen as the baseline material for this study. They are designated as Type A-1 and Type A-4 fibers (Hercules, Inc.). The fibers have a tensile modulus of about 35 Msi and a tensile strength of about 425 ksi. Figure 1 shows scanning electron micrographs of the two fibers. Both fibers are circular in cross section. However, the A-1 fiber has longitudinal, discontinuous topographical ridges extending parallel to the fiber axis on its surface while the A-4 fiber has a microscopically smooth surface. The fibers were supplied by the manufacturer untreated (AU-1 and AU-4), untreated

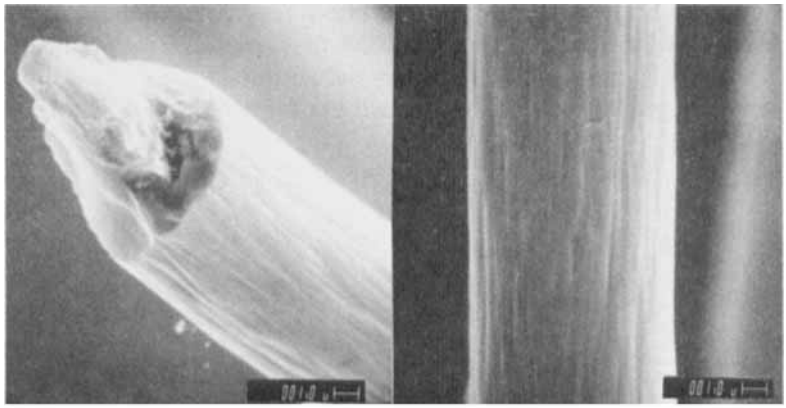

AS-1 Fiber

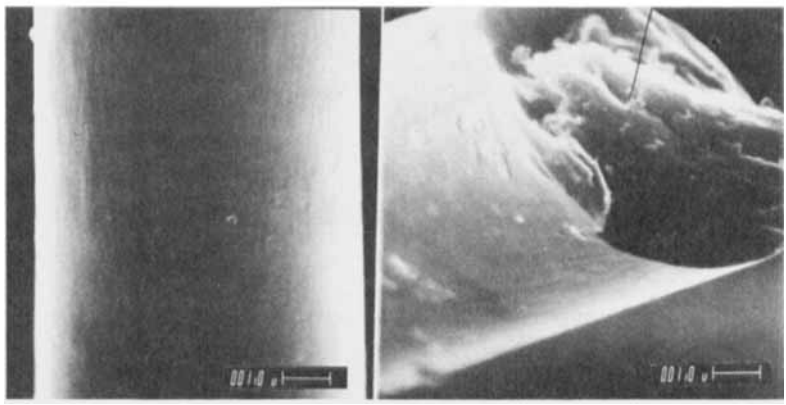

AS-4 Fiber

FIGURE 1 Scanning Electron Micrograph of the AS-1 and AS-4 Graphite Fibers Showing the Differences in Topography.

but coated with DER-330, a diglycidyl ether of bisphenol-A (Dow Chemical Co.), to 100–200 nm thickness (AU-1C and AU-4C), surface treated (AS-1 and AS-4) and surface treated and coated with 100-200 nm of DER-330 epoxy resin (AS-1C and AS-4C). A previous study measured surface areas of fibers produced in a similar manner and concluded that an increase in surface area does not accompany the fiber surface treatment used here.[4,5] The fibers were examined for

uniformity of finish throughout the fiber tow. The scanning electron micrograph of Figure 2 shows that all fibers were uniformly coated with a thin layer of epoxy. Those on the outside of the tow did, however, have areas where the resin finish has formed droplets.

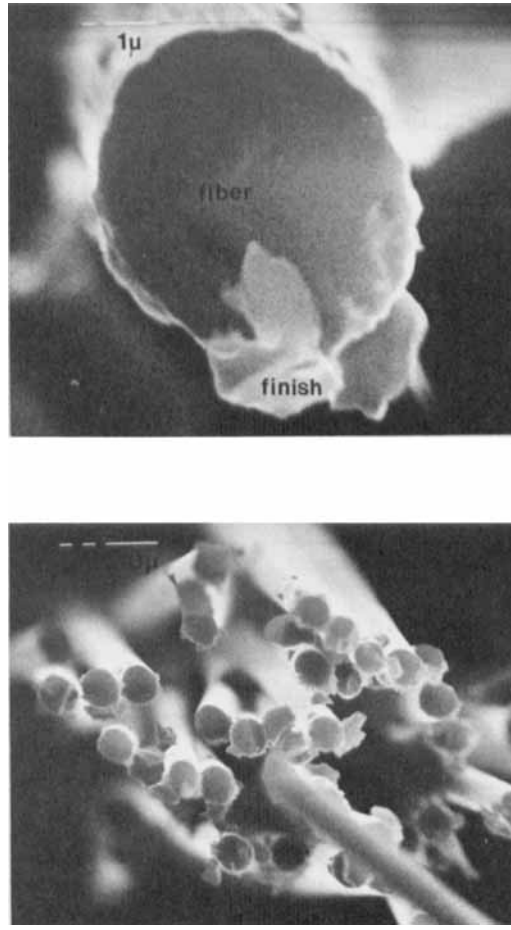

FIGURE 2 Scanning Electron Micrograph of the AS-1C Graphite Fiber with the 100–200 nm Diglycidyl Ether of Bisphenol-A Finish Layer.

B. Matrix

The matrix used in this investigation was a stoichiometric mixture of a diglycidyl ether of bisphenol-A (Epon 828, Shell Chemical Co.) cured with 14.5 phr meta-phenylene diamine (m-PDA, Aldrich Chemical Co.). The m-PDA was of high purity and was kept in a cool, dark, inert environment to prevent deterioration. A previous study has shown that a "darkened" m-PDA can affect the interfacial properties while leaving the bulk properties of the epoxy unchanged.[6] The Epon 828 was likewise kept in a cool, inert environment to prevent deterioration during the course of these experiments. The Epon 828 is very similar to the DER-330 epoxy used as the finish. The matrix system was vacuum melted and debulked and then processed for two hours at 75°C and for two hours at 125°C followed by an overnight cooldown.

C. Interfacial Shear Strength

The adhesion between fiber and matrix was characterized through measurement of the interfacial shear strength. This is accomplished by embedding the fiber in a tensile coupon of matrix resin and subjecting the specimen to tensile loading. Since the tensile forces are transferred to the fiber through shear forces at the fiber-matrix interface and because the maximum strain of the fiber is much less than that of the matrix, the fiber will fracture into small segments within the matrix. As higher tensile loads are applied the fracture process continues until the interfacial forces no longer induce fracture in the fiber. At this point a minimum segment length is attained known as the critical transfer length which allows the interfacial shear strength to be determined.

The relationship between fiber tensile strength (σ_f), critical length to diameter ratio (l_c/d) and the interfacial shear strength (τ) is given by

$$\tau = \frac{\sigma_f d}{2l_c} \tag{1}$$

Since a distribution of lengths is observed experimentally, this relationship has been altered to reflect Weibull statistics to the form

$$\tau = \frac{\sigma_f}{2\beta}\Gamma\left(1 - \frac{1}{\alpha}\right) \tag{2}$$

where (α) is the shape factor, (β) is the scale factor (*i.e.*, the mean value of l_c/d) and (Γ) is the Gamma function. This relationship is used to evaluate the interfacial shear strength between fiber and matrix. Details of the technique and the data accumulation and reduction schemes have been published.[7]

D. Microscopy

Two microscopic techniques were used to investigate the interfacial response between graphite fiber and matrix as a function of both shear loading and surface finish. Optical microscopy with transmitted polarized light was used to detect fiber fracture within the epoxy specimen and to document the load transfer from fiber to matrix near the region of the fiber break. Transmitted electron micrographs (TEM) of 70 nm thick sections of graphite fiber-epoxy specimens cut parallel to the fiber axis with an ultramicrotome were used to document the failure path at the interface. Details of the techniques have been published.[1]

E. Fiber Surface Analysis

Analysis of the fiber surface chemical composition was conducted by means of x-ray photoelectron spectroscopy (XPS), also known as ESCA. Measurements were made using a KRATOS ES300 XPS system equipped with a magnesium x-ray source. The analyzer was set at a fixed pass energy of 65 eV and a resolution (ΔE) of 0.25 eV for these analyses. Data was accumulated in the pulse counting mode on an LSI-11/03 minicomputer. Peak binding energies were calibrated using 284.6 eV for the C_{ls} peaks. Surface compositions were calculated using integrated peak areas which were corrected for photoelectric cross-section,[8] analyzer transmission[9] and electron mean-free path.[10]

The accuracy of the surface concentration values on an absolute basis is dependent on the assumptions used in reducing the spectra. For these fibers the surface concentration values are estimated to be accurate to +/− 20 percent. The standard deviation of this group of measurements is +/−1 atomic percent for each element. Expressed as a percentage, the standard deviations ranged from 2% for carbon to 100% for sodium.

3. RESULTS

A. XPS Analysis

A summary of the XPS results is presented in Table I. Data of the A-1 series of fibers was the same as for the A-4 series of fibers within experimental error. The table lists only one set of data which applies equally to each fiber set except where noted.

TABLE I
XPS Analysis of A-1 and A-4 Graphite Fibers

Fiber	*Carbon 1s*			*Oxygen 1s*			*Nitrogen 1s*	*Sodium 1s*
	B.E.	*FWHM*	*At. %*	*B.E.*	*FWHM*	*At. %*	*At. %*	*At. %*
	(eV)	(eV)		(eV)	(ev)			
AS	284.6	1.7	85	532.5	3.1	10	4.5*	1.0
	286.4							
	288.7							
ASC	284.6	2.3	88	532.9	1.7	11	0.4	0.6
	286.2							
ASC	284.6	1.9	83	532.9	2.4	13	3.0**	1.0
(MEK ext)	286.4							
	288.7							

*4.0% for AS4 **2.5% for AS4C

Representative scans of the carbon and oxygen photoelectron peaks from these three sample groups are shown in Figure 3. The carbon 1s peak from the AS fiber specimen suggests the presence of three components. The major component is due to carbon-carbon single bonding at a binding energy of 284.6 eV. A smaller peak at 286.6 eV is due to carbon-oxygen bonding and a peak at 288.7 eV is due to carboxylic type carbon-oxygen complexes. The oxygen 1s spectrum is broad suggesting that more than one component is present. Compositionally, the surface of the AS fiber has about ten percent oxygen, four and one-half percent nitrogen and some sodium detectable at less than one percent. The remainder of the surface is carbon.

The spectra of the ASC (epoxy coated) fibers are quite different from the spectra of the AS fibers. The carbon 1s peak exhibits only two components instead of three (the small peak at 291 eV is a loss peak due to the presence of aromatic carbons). These two components are due to carbon-carbon type bonds at 284.6 eV and carbon-oxygen bonds

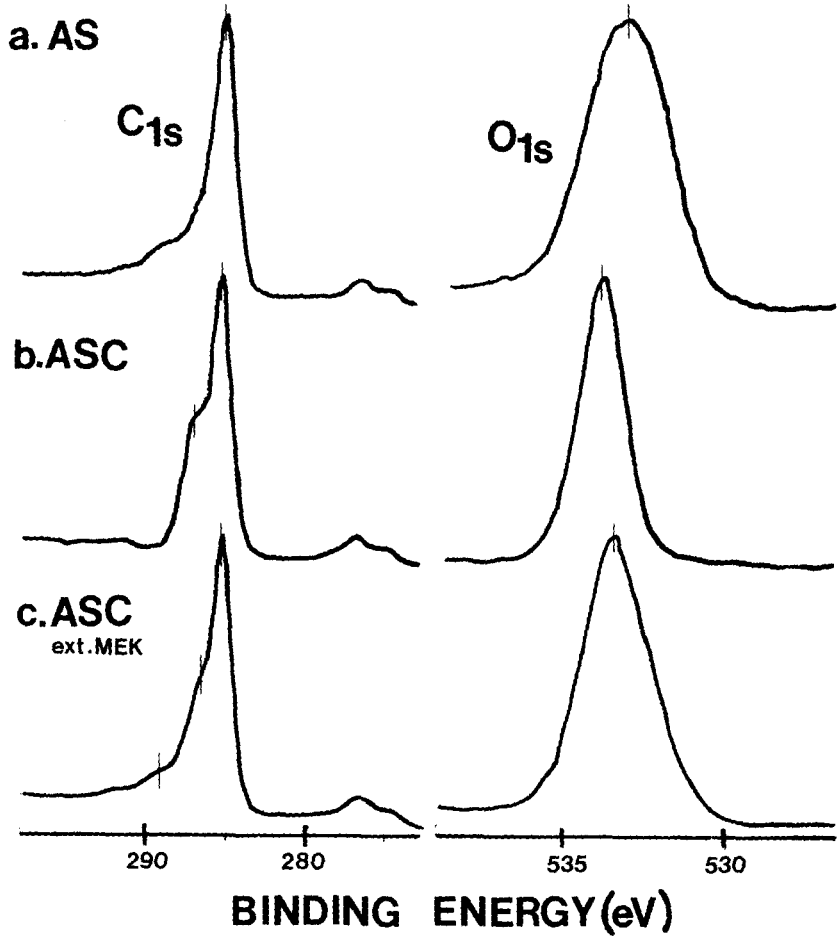

FIGURE 3 XPS Spectra of C_{1s} and O_{1s} Photoelectron Peaks from a) AS, b) ASC and c) ASC extracted with MEK Fiber Samples. (Peak positions are not corrected for charging.)

at 286.2 eV. The oxygen 1s peak is shifted 0.4 eV higher in binding energy and is much narrower than that found on the AS fiber. This correlates well with the absence of the carboxylic component of the carbon 1s peak at 288.7 eV, since the doubly-bonded oxygen would be found at a lower binding energy and is consistent with the known structure of the DGEBA molecule. Spectra obtained on thick films

of the DGEBA cast from solvent are quite similar to the spectra obtained here. The very low atomic percent of nitrogen and sodium detected on the ASC fiber surface indicates that the original AS fiber surface is completely covered by the finish layer.

The ASC fiber was placed in a Soxhlet extractor with methyl ethyl ketone (MEK) for 100 hours to remove the epoxy finish that was not chemisorbed to the fiber surface. The maximum temperature seen by the fiber during this extraction and in the subsequent drying operation was 75°C. The extraction with methyl ethyl ketone (MEK ext) produces a fiber surface that exhibits an XPS spectrum that has features of both the AS and ASC spectra. There are three carbon 1s components, but present in different intensities, from the AS surface. The oxygen 1s spectrum is again shifted to higher binding energy but now has a definite broadening of the low energy side. The full widths at half maximum (FWHM) for both peaks are between those of the AS and ASC fibers. The surface concentration of oxygen is slightly greater than that obtained for the AS fiber before the application of the finish. This is most probably due to retention of some epoxy on the fiber surface whose oxygen content contributes to the total surface oxygen level. The nitrogen intensity is reduced from that found on the AS fiber. This also suggests that these atoms are not detected due to epoxy adsorption on the surface even after extraction. Overall, it can be concluded that some small amount of epoxy remains on the ASC fiber after extraction with methyl ethyl ketone.

B. Interfacial Shear Strength

Table II lists the tabulated data for the interfacial shear strength for each fiber and treatment tested in the EPON 828-mPDA matrix.

TABLE II
Interfacial Shear Strength (τ) for Graphite Fibers in EPON 828/mPDA

Fiber	$\sigma_f(l_c)$	β	α	τ (*ksi*)
AU-1	630ksi	70.1	2.6	6.5
AU-1C	645ksi	50.8	3.2	8.4
AS-1	655ksi	38.8	3.5	10.8
AS-1C	665ksi	30.3	3.8	13.6
AU-4	830ksi	99.5	3.3	5.4
AU-4C	840ksi	86.3	3.8	6.1
AS-4	845ksi	57.2	3.1	9.9
AS-4C	850ksi	43.8	4.1	11.8

Fiber tensile strengths ($\sigma_f(l_c)$) are given at the critical length for each fiber. The values for the fiber tensile strength have been interpolated from semi-log plots of the fiber tensile strength as a function of gauge length. The Weibull parameters (α) and (β) that were determined from the experimental data are listed as well as the interfacial shear strength (τ) calculated with the use of Equation 2. The coefficient of variation for the value of the interfacial shear strength was determined to be between 0.1 and 0.2.

Within either the A-1 fiber or the A-4 fiber data, parallel increases in the interfacial shear strength are observed. The coated untreated fibers have a greater τ than the uncoated untreated fibers for both fiber types. Likewise the coated surface treated fibers have a larger τ than the uncoated surface treated fibers for both sets. The ratio of the interfacial shear strength for the coated fiber to that of the same fiber without the finish varies between 1.13 and 1.30 for all the fibers investigated in this study.

C. Failure Mode

The photoelastic stress patterns exhibited by the epoxy near the ends of the fiber fragments created during the interfacial shear strength measurements were recorded as a function of increasing sample strain. Figure 4 is a composite of polarized transmitted light micrographs of each of the fibers with their indicated surface treatment-finish combinations for the A-1 fiber. the results for the A-4 fiber are shown in Figure 5. The micrographs were taken at 400x at the fiber breaks while the samples were under $\sim 4\%$ strain. Immediately adjacent to each polarized micrograph is the associated transmitted light micrograph at the same magnification. The fiber break is centered in all of the micrographs of Figures 4 and 5.

The behavior of each fiber in the matrix changes with the surface treatment and/or finish associated with it. Both untreated fibers (*i.e.*, AU-1 and AU-4) exhibit low intensity diffuse polarized light micrographs in the region around the fiber break. As the specimen is stressed the photoelastic region rapidly expands and encompasses the whole fiber fragment. During this process the photoelastic region expands in a stick-slip manner with increasing strain. The alternating light and dark regions are due to this stick-slip type behavior. The transmitted light micrograph shows fiber separation at the break with increasing strain (region between arrows).

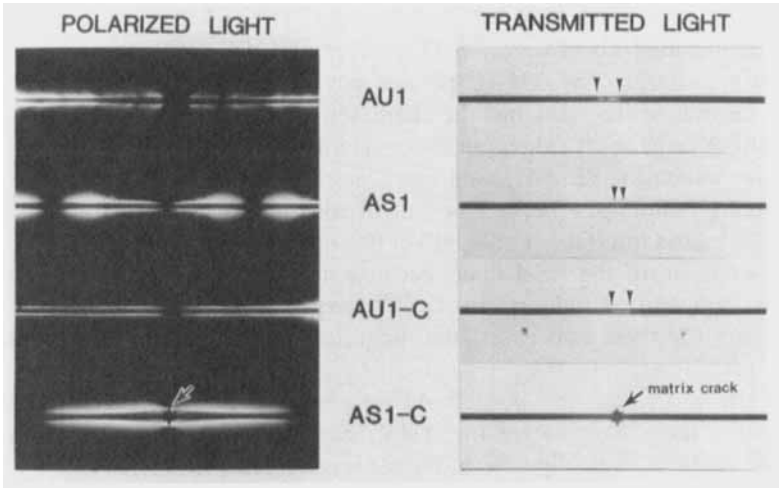

FIGURE 4 Polarized and Transmitted Light Micrographs (400X) of the AU-1, AU-1C, AS-1 and AS-1C Graphite Fibers at ~4% Strain in the Epoxy Matrix.

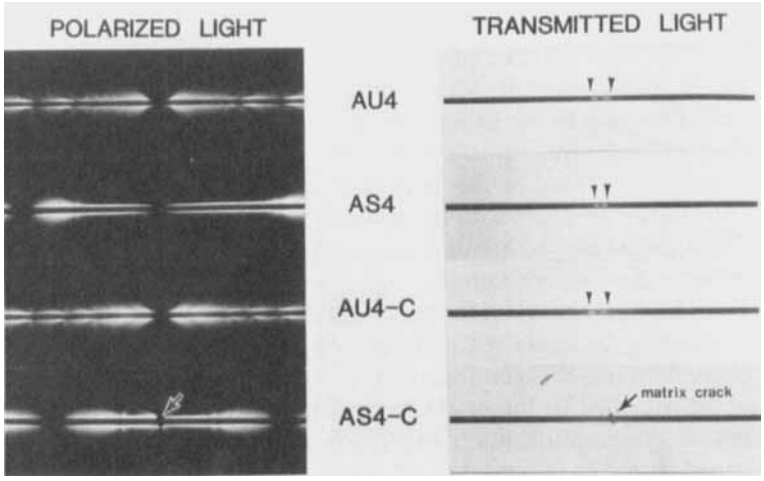

FIGURE 5 Polarized and Transmitted Light Micrographs (400X) of the AU-4, AU-4C, AS-4 and AS-4C Graphite Fibers at ~4% Strain in the Epoxy Matrix.

The untreated but coated fibers (*i.e.*, AU-1C) and the surface treated but uncoated fibers (*i.e.*, AS-1) give remarkably similar photoelastic stress patterns. The AU-1C pattern covers a fragment length almost twice that of the AS-1 but the characteristic features are the same for both. A large spherical region appears immediately after the fiber break. With increasing sample strain this region moves away from the break leaving behind a very narrow but intense photoelastic region at the fiber-matrix interface. The length of this region is greater for the AU-1C fibers than for the AS-1 fibers because of their greater critical length. The transmitted light micrograph shows that while fiber separation occurs for these two cases, the magnitude of separation with strain is much lower.

The untreated and coated AU-4C exhibits a photoelastic stress pattern more like that of the AU-4 than that of the AS-4, as in the A-1 series. A stick-slip type of failure is observed with increasing load. The surface treated but uncoated AS-4 gives a photoelastic stress pattern almost identical to the AS-1. The failure of the AU-4C fiber to behave in a similar fashion to the AU-1C is most probably due to the difference in topography. The convoluted AU-1C surface may contribute to the shear strength of the interface while the microscopically smooth AU-4C surface may not.

The surface treated and coated fibers (AS-1C and AS-4C) give very intense photoelastic stress patterns. The interfacial shear strength of these fibers is the highest and the growth of a matrix crack perpendicular to the fiber can be detected at the fiber breaks as seen in the transmitted light micrograph. Matrix cracking at the fiber break was not observed for any of the other fiber specimens.

Figures 6–9 are transmission electron micrographs of ultramicrotomed sections of the indicated samples. Sections were made parallel to the fiber axis with the knife direction indicated by the arrow in the micrographs. Sectioning was completed after straining in order to observe the locus of failure at the fiber breaks.

The TEM for the AU fiber is not shown. The interface between the AU fiber and the epoxy matrix discussed in previous work shows that interfacial failure between fiber and matrix occurs.[1] Fragments of the fiber are attached to the epoxy indicating that failure is in the outer layers of the graphite fiber. Figures 6 and 7 show typical sections obtained with AU-1C and AU-4C fibers. Graphite fiber fragments are visible in the micrograph attached to the epoxy matrix side of the interface after failure. The presence of the coating although increasing

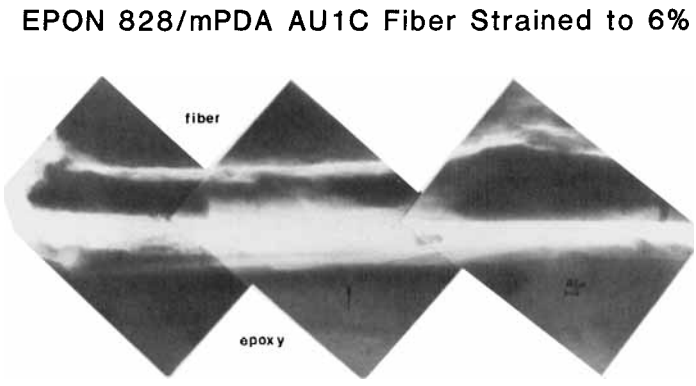

FIGURE 6 Transmission Electron Micrograph of an Ultramicrotomed Section of the AU-1C/Epoxy Interphase after Straining. (The knife direction is shown by the arrow and is perpendicular to the interface.)

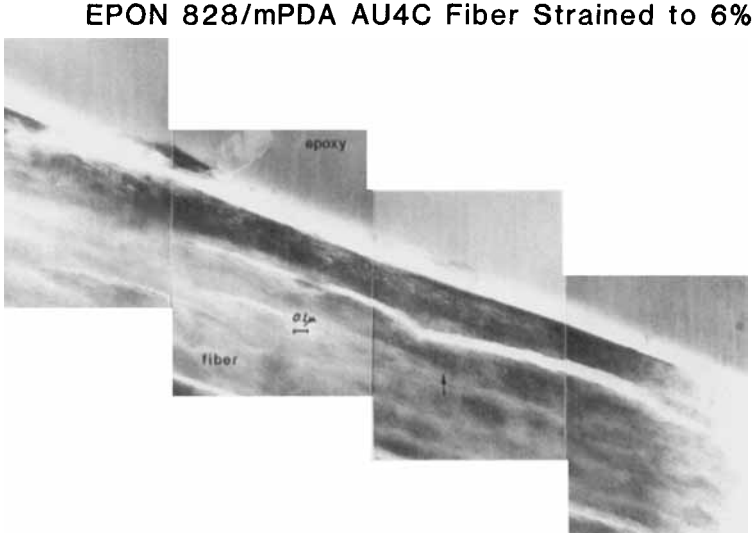

FIGURE 7 Transmission Electron Micrograph of an Ultramicrotomed Section of the AU-4C/Epoxy Interphase after Straining. (The knife direction is shown by the arrow and is perpendicular to the interface.)

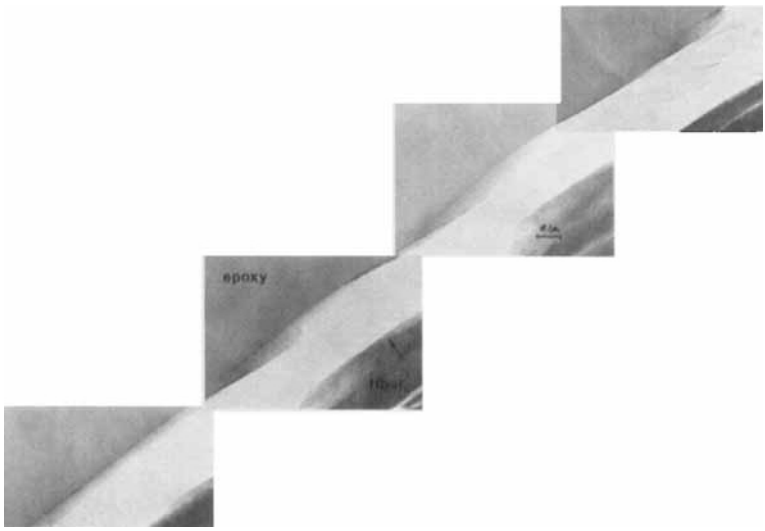

FIGURE 8 Transmission Electron Micrograph of an Ultramicrotomed Section of the AS-1/Epoxy Interphase after Straining. (The knife direction is shown by the arrow and is perpendicular to the interface.)

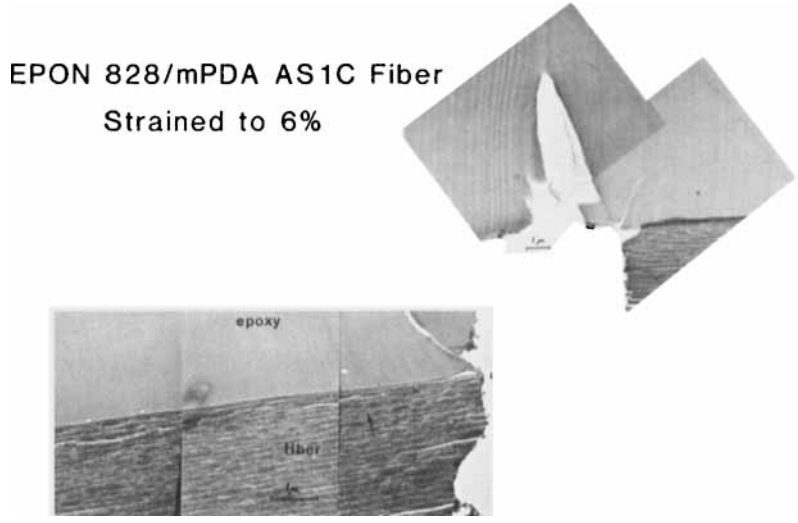

FIGURE 9 Transmission Electron Micrograph of an Ultramicrotomed Section of the AS-1C/Epoxy Interphase after Straining. (The knife direction is shown by the arrow and is perpendicular to the interface.)

the interfacial shear strength does not alter the failure path from that obtained with the AU-1 or AU-4 fiber in the same matrix.

The AS-1 fiber likewise fails interfacially under shear stress (Figure 8). Previous work[1] has shown that an interfacial crack propagates from the fiber break along the fragment length with increasing applied stress. For this surface treated fiber however, the failure path is strictly interfacial with no evidence of fiber failure in the outer layers as seen with the AU fiber. Application of the finish to this fiber causes a dramatic change in behavior as seen in Figure 9, the TEM for the AS-1C fiber. In this case, matrix fracture perpendicular to the fiber surface at the fiber breaks takes place instead of interfacial failure. The microtomed sections show that interfacial crack growth does not take place.

4. DISCUSSION

The results of this investigation have shown that the presence of the 100–200 nm epoxy finish increases the interfacial shear strength between fiber and matrix and also changes the failure mode from interfacial to matrix. There are four possible explanations for the effect of the fiber finish on interfacial behavior.

Damage Protection. Graphite fibers are brittle materials and are therefore susceptable to strength degradation due to the presence of surface flaws. Handling operations, where fiber to fiber contact is present, can introduce surface flaws which would reduce fiber and composite properties. It has been speculated that the fiber finish is beneficial because it prevents fiber to fiber contact and hence the introduction of surface flaws.

If the primary function of the fiber finish is to protect the surface from flaws generated by the normal handling procedures, a reduction in tensile properties of the fiber would be observed in the uncoated fibers but not in the coated ones. This is not observed. Within statistical error the fiber strengths of all four samples are unchanged by the presence of the coating. (*i.e.*, AU-1 = AU-1C, AS-4 = AS-4C, *etc.*) This is true at both the 25 mm gage length and at the much shorter critical lengths. (see Table 2)

Wettability. From a composite viewpoint, complete and thorough infiltration and wetting of the twelve-thousand-filament tows is a necessary condition for good composite properties. Unwetted regions act as stress concentrations which degrade composite performance. The

application of a matrix compatible finish might enhance wetting of the fibers by the matrix and be responsible for the improvement in interfacial shear strength.

Contact angle and surface free energy measurements on the fibers and epoxy matrix used in this study do not indicate that wettability changes would be significant. The fibers used in this work have surface free energies which are greater than the surface free energy of the epoxy and the epoxy/curing agent mixture (*i.e.*, fibers > 50 mJ/m^{2}vs. epoxy < 50 mJ/m^2).[11] The pure epoxy itself has a value of surface free energy that is about the same as that of the epoxy mixture.[12] The epoxy resin is, of course, soluble in the epoxy mixture and undoubtedly this insures good wetting and infiltration. Thermodynamically the presence of the finish alone would not be expected to favor better adhesion.

Enhanced Surface Reactivity. Application of a fiber finish may be beneficial to fiber-matrix adhesion through the creation of a protective environment for the reactive surface groups added to the fiber surface with treatment. Normally fibers are produced and surface treated and then wound on a spool for shipment to a composite prepreg or fabrication facility. Environmental exposure might reduce the reactivity of the beneficial surface groups.

Thermal desorption-mass spectroscopic studies of the fibers used in this study have shown that the equivalent of up to three monolayers of water, carbon monoxide and carbon dioxide can be desorbed from these surfaces at temperatures less than 150°C, indicating physical adsorption of atmospheric gases.[4,5] XPS studies as AS fibers manufactured five years apart, on the other hand, show little difference in either quantity or character of the surface species. The XPS analysis of these fibers without the finish and those that have had the finish extracted with MEK show very little difference as shown by the data in Table 1. The few percent of the fiber surface that has retained the epoxy after extraction and which may therefore be inferred as being chemisorbed, would not be responsible for the 25% increase in interfacial shear strength. Indeed, a reduction by 80% in surface oxygen species on this same fiber produced only a few percent decrease in interfacial shear strength.[1] Horie *et al.*[13] have attempted to determine the chemical bonding of the epoxy matrix cured with an amine to graphite fibers. They propose that hydrogen bonding between the carboxylic surface groups of the fiber and the amine group of the resin occurs at low temperatures (*i.e.*, 60°C). Since the pure DGEBA epoxy layer

prevents amine from coming in contact with the fiber surface, chemical interaction between them is prevented here.

Creation of an Interphase. The application of a fiber finish can create an interphase layer around the fiber which could affect the fiber-matrix adhesion. Figure 10 is a schematic drawing in quarter view of the fiber and polymer in the interfacial region. Initially the fiber has a 100–200 nm finish of pure DGEBA epoxy resin without amine curing agent (Figure 10a). This has been applied from solvent and dried at low temperatures, *i.e.*, < 100°C. Homopolymerization of the epoxy has not been observed under these conditions.[14] This coated fiber is then placed in a stoichiometric mixture of DGEBA with the proper amount of amine curing agent, in this case 14.5 phr. During the 50 minutes before gelation the amine is free to diffuse into the amine free finish at the same time that it is reacting with epoxy functionalities. This would retard free diffusion and create an interphase layer larger than the 100–200 nm finish having a gradation in amine concentration decreasing from the bulk of the resin to a very low value near the fiber surface (Figure 10b). Whatever amine concentration gradient exists in the interphase, it would have less than the stoichiometric amount necessary for full cure under these conditions. Kardos[15] has detected the presence of an interphase in many composite systems including a glass-Epon 828 composite.

It is not currently possible to determine the mechanical properties

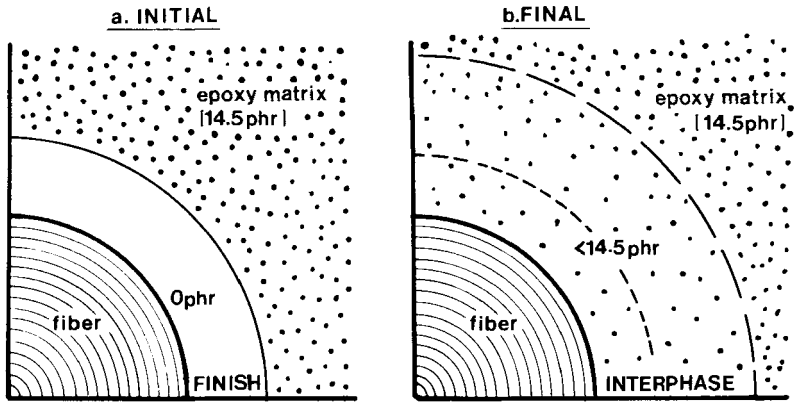

FIGURE 10 Schematic diagram of the Interphase Region, a) at the Initial Moment of Fabrication and b) after Final Cure.

of a polymer region of microscopic dimensions as studied here. Therefore, an attempt was made to determine the properties of this region with reduced curing agent by measuring the properties of mixtures of EPON 828 with varying amounts of mPDA cast and cured under identical conditions to those used to fabricate the single fiber specimens. Figure 11 is a plot of the Young's tensile modulus, (E_y), fracture strength (σ_f) and fracture toughness (K_{1c}) of these epoxy variations. The modulus reported is the initial modulus determined from strain-gaged samples and the fracture toughness was determined using the compact tension specimen at room temperature and a strain rate of 0.002 inches per minute. Comparing the epoxy with less than the stoichiometric amount of curing agent to the stoichiometric amount at 14.5 phr indicates that reducing amine content results in a material with a higher modulus, lower fracture stress and lower fracture toughness. This indicates that the interphase region would be expected to behave as a more brittle

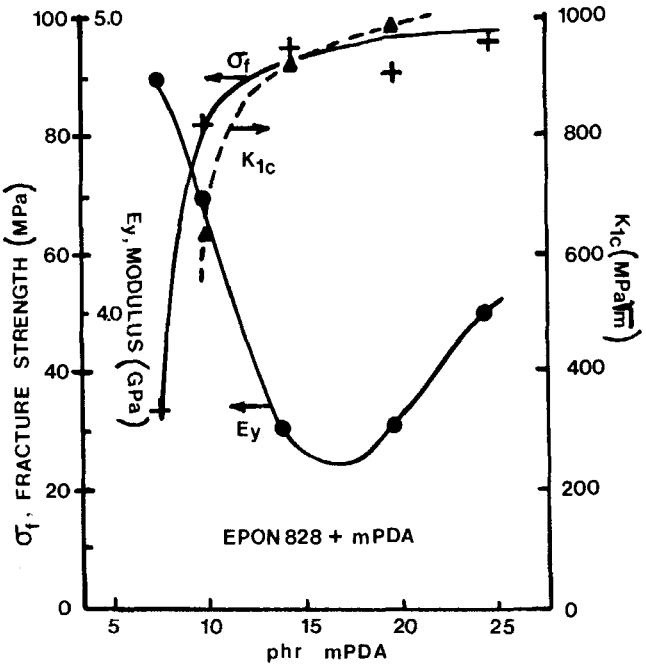

FIGURE 11 Initial Tensile Modulus (E_y), Fracture Strength (σ_f) and Fracture Toughness (K_{1c}) of Epon 828/mPDA Mixtures as a Function of Parts per Hundred Resin (phr) of mPDA.

material than the stoichiometric epoxy. Identical results have been documented in the literature for similar amine cured systems. [16,17]

The presence of material of higher modulus itself can have an effect on the stress transfer and consequently the interfacial shear strength. Kelly and Tyson[18] compared the effect of an elastic/plastic matrix versus an elastic matrix on the value of critical length for a given fiber. They showed that a material of higher modulus increases the shear stress transfer at the interface and thereby reduces the critical transfer length giving rise to an increase in the interfacial shear strength calculated by this single filament method. Others[19,20] have derived mathematical relationships for a model single fiber fragment system which show that the interfacial shear strength increases with the shear or tensile modulus of the interphase.

In addition to the increase in interfacial shear strength, the brittle finish layer has a lower fracture toughness. Stress concentrations exist at the fiber breaks[21] which can cause initiation of fracture to occur at the fiber breaks and to grow perpendicular to the fiber axis into the matrix instead of along the fiber-matrix interphase. This can be seen in the micrographs of Figures 4 and 5 for the AS-1C and the AS-4C fibers. Because fiber to fiber distance in an actual composite is on the order of a fiber diameter or less, the presence of a matrix crack perpendicular to the fiber surface would be expected to reduce fracture toughness properties of the composite when a finish layer is present on the fiber.

5. CONCLUSIONS

The application of a resin finish to graphite fibers has a two-fold effect. First, there is an increase in the interfacial shear strength between fiber and matrix. Second, the mode of failure at the fiber break is altered from growth of an interfacial crack between fiber and matrix to that of a matrix crack perpendicular to the fiber axis.

The mechanism by which this epoxy finish affects both the adhesion and failure mode is through the creation of a brittle interphase around the fiber. The finish layer contains less than the stoichiometric amount of curing agent and creates a layer having a higher modulus along with a lower fracture toughness. This in turn promotes better stress transfer resulting in a higher interfacial shear strength but because of the lower fracture toughness, the failure mode changes from interfacial to matrix.

Acknowledgements

The authors wish to thank Ken Lindsay of the University of Dayton Research Institute for making the fiber tensile strength measurements at various gage lengths and Dr. W. B. Jones for the determination of the neat resin fracture toughness.

References

1. L. T. Drzal, M. J. Rich and P. F. Lloyd, *J. Adhesion* **16**, 1 (1983).
2. W. A. Fraser, F. H. Ancker and A. T. DiBenedetto, *Proc. of 1975 Conf. of RP/Composites Inst.*, Paper 22-A, (1975).
3. J. C. Goan, L. A. Joo and G. E. Sharpe, *Proc. of 1972 Conf. of RP/Composites Inst.*, Paper 21-E, (1972).
4. L. T. Drzal, *Carbon* **15**, 129 (1977).
5. L. T. Drzal, J. A. Mescher and D. L. Hall, *Carbon* **17**, 375 (1979).
6. K. Gutfreund and D. Kutscha, *Interfacial Investigations in Advanced Fiber Reinforced Plastics*, AFML-TR-67-275, 59 (1967).
7. L. T. Drzal, M. J. Rich, J. P. Camping and W. J. Park, *Proc. of 1980 Conf. of RP/Composites Inst.*, Paper 20-C, (1980).
8. J. H. Scofield, *J. Elec. Spectros. Rel. Phen.* **8**, 129 (1976).
9. H. D. Polaschegg, *Appl. Phys.* **4**, 63 (1974).
10. C. J. Powell, *Surf. Sci.* **44**, 29 (1974).
11. G. E. Hammer and L. T. Drzal, *Appl. Surf. Sci.* **4**, 340 (1980).
12. F. Weaver, *Epoxy Adhesive Surface Energies Via the Pendant Drop Method*, Air Force Wright Aeronautical Laboratories Technical Report, AFWAL-TR-82-4179, (1982).
13. K. Horie, H. Murai and I. Mita, *Fibre Sci. Tech.* **9**, 253 (1976).
14. H. Lee and K. Neville, *Handbook of Epoxy Resins* (McGraw-Hill, NY, 1967).
15. J. L. Kardos, *Trans. N.Y. Acad. Sci., II* **35**, 136 (1973).
16. K. Selby and L. E. Miller, *J. Mater. Sci.* **10**, 12 (1975).
17. S. L. Kim, *et al.*, *Poly. Engr. and Sci.* **18**, 1093 (1978).
18. A. Kelly and W. R. Tyson, *J. Mech. Phys. Solids* **13**, 329 (1965).
19. B. D. Agarwal and R. K. Bansal, *Fibre Sci. Tech.* **12**, 149 (1979).
20. B. W. Rosen, *Fibre Composite Materials* (American Society for Metals, 1965).
21. J. M. Mahishi and D. F. Adams, *J. Mater. Sci.*, (in press).